Multiple charge-density waves in $R_5Ir_4Si_{10}$ (R=Ho, Er, Tm, and Lu)

Sander van Smaalen,[1,*] Mohammad Shaz,[1] Lukas Palatinus,[1] Peter Daniels,[1] Federica Galli,[2] Gerard J. Nieuwenhuys,[2] and J. A. Mydosh[2,†]

[1]*Laboratory of Crystallography, University of Bayreuth, 95440 Bayreuth, Germany*

[2]*Kamerlingh Onnes Laboratory, University of Leiden, Leiden, The Netherlands*

(Received 7 October 2003; published 22 January 2004)

The charge-density-wave (CDW) transitions in compounds $R_5Ir_4Si_{10}$ (R=rare-earth element) have been studied by x-ray-diffraction and electrical conductivity experiments for temperatures between 20 and 300 K. At T_{CDW} incommensurate CDW's [$\vec{q}=(\pm 0.25\pm\delta)\vec{c}^*$ with $\delta\approx 0.03$] develop in compounds with R=Ho, Er, Tm, and ($Lu_{0.16}Er_{0.84}$), while commensurate CDW's [$\vec{q}=(n/7)\vec{c}^*$] develop in compounds with R=Lu and ($Lu_{0.34}Er_{0.66}$). T_{CDW} varies between 83 K in R=Lu and 161.4 K in R=Ho. The compounds with an incommensurate CDW exhibit a second transition at $T_{lock\text{-}in}<T_{CDW}$, with $T_{lock\text{-}in}$ between 55 K in R=Er and 111.5 K in R=Tm. In $Ho_5Ir_4Si_{10}$ and $Er_5Ir_4Si_{10}$ this is a pure lock-in transition at which δ becomes zero. In $Tm_5Ir_4Si_{10}$ and $(Lu_{0.16}Er_{0.84})_5Ir_4Si_{10}$ δ also becomes zero, but below $T_{lock\text{-}in}$ additional satellite reflections have been discovered, at commensurate positions $(n/8)\vec{c}^*$ in $Tm_5Ir_4Si_{10}$ and at incommensurate positions $(n/8\pm\delta_2)\vec{c}^*$ with $\delta_2\approx 0.01$ in $(Lu_{0.16}Er_{0.84})_5Ir_4Si_{10}$. The development of this second CDW can be understood by a two-step mechanism similar to the mechanism for the development of the primary CDW in $Er_5Ir_4Si_{10}$ [Galli *et al.*, Phys. Rev. Lett. **85**, 158 (2000)]. At $T_{lock\text{-}in}$ the primary CDW becomes commensurate, leading to a partly restoration of the Fermi surface, as evidenced by an anomalous decrease of the electrical resistivity for T below $T_{lock\text{-}in}$ in $Ho_5Ir_4Si_{10}$ and $Er_5Ir_4Si_{10}$. The modified Fermi surface then provides the favorable nesting conditions for the development of a second CDW in $Tm_5Ir_4Si_{10}$ and $(Lu_{0.16}Er_{0.84})_5Ir_4Si_{10}$. The electronic character of this transition is suggested by the anomalous increase of the resistivity for T below $T_{lock\text{-}in}$.

DOI: 10.1103/PhysRevB.69.014103 PACS number(s): 61.44.Fw, 71.45.Lr, 64.70.Rh, 61.50.Ks

I. INTRODUCTION

Compounds with low-dimensional electronic bands have been extensively studied because of their qualitatively different behavior than three-dimensional (3D) systems.[1] Typical phenomena in low-dimensional electronic systems include Luttinger liquid behavior as opposed to Fermi-liquid behavior in 3D systems, and the development of charge-density waves (CDW's) and spin-density waves.[2,3]

Rare-earth metal (R) transition metal silicides $R_5Ir_4Si_{10}$ exhibit CDW transitions at temperatures T_{CDW} in the range 80 K$<T_{CDW}<$210 K, depending on the rare-earth element R.[4–6] Anomalies at T_{CDW} have been observed in the temperature dependencies of the electrical conductivity, specific heat, thermopower, thermal conductivity, thermal expansion, and elastic constants.[4,5,7–10] The CDW character is suggested by the fact that these anomalies are in agreement with a decrease of the densities of states (DOS) at the Fermi level. Furthermore, weak satellite reflections in the x-ray diffraction have been found to develop below T_{CDW}.[8,11] The transitions in compounds $R_5Ir_4Si_{10}$ are unconventional CDW transitions, as exemplified by the sharpness of the anomalies and by the very small anisotropy of the electrical conductivity.[8,10,12] This has led to the interpretation that these compounds are CDW systems with strong interchain coupling.[8]

A second special feature of these CDW systems is the presence of f electrons on the rare-earth atoms. The f electrons are responsible for localized magnetic moments, and at temperatures far below T_{CDW} phase transitions from paramagnetic to antiferromagnetic (AF) states have been found.[6,13] Alternatively, nonmagnetic compounds, e.g. with R = Lu, become superconducting at low temperatures.

The interplay between CDW's and superconductivity has been demonstrated by the temperature-pressure phase diagram of $Lu_5Ir_4Si_{10}$. At ambient pressure $T_{CDW}=83$ K and superconductivity develops below $T_{sc}=3.9$ K.[4,14] Increasing the pressure gradually suppresses the CDW transition until it suddenly disappears above $p_0=2.1$ GPa. Up to this pressure T_{sc} is nearly constant, but it jumps from 3.8 K below p_0 towards 9 K at higher pressures. These observations are explained by assuming that the CDW transition removes part of the DOS at the Fermi level, thus reducing T_{sc}.[4] At the same time this model supports the CDW partial gapping character of the transition at T_{CDW}.

The coexistence of AF order and a CDW was established in $Er_5Ir_4Si_{10}$ by the simultaneous observation of CDW satellite reflections and resonant magnetic superlattice reflections in x-ray diffraction below $T_N=2.8$ K.[15] The interplay between these two phenomena is suggested by comparing the behaviors of $R_5Ir_4Si_{10}$ and isostructural $R_5Rh_4Ge_{10}$. The magnetic transition temperatures T_N are higher in the latter compounds than in the former ones, while the absence of CDW transitions has been established in $R_5Rh_4Ge_{10}$.[16] Apparently, the CDW in $R_5Ir_4Si_{10}$ removes DOS at the Fermi level, that when present in other compounds, such as $R_5Rh_4Ge_{10}$, causes an increased Ruderman-Kittel-Kasuya-Yosida interaction between the localized, magnetic f electrons. The interactions between conduction electrons and f electrons may also be responsible for the unconventional characters of the CDW's and CDW transitions as compared to the properties of conventional CDW systems.

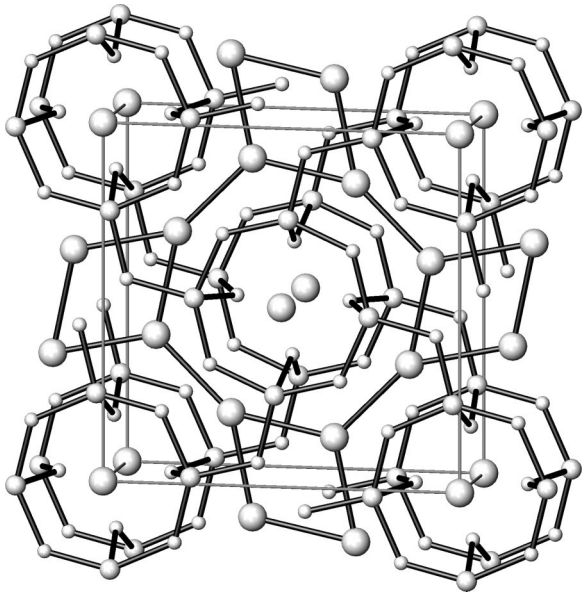

FIG. 1. Perspective view of the basic structure of $R_5Ir_4Si_{10}$ along the tetragonal c axis. Large circles represent R atoms, intermediate circles are Ir, and small circles denote Si.

The compounds $R_5Ir_4Si_{10}$ crystallize in the $Sc_5Co_4Si_{10}$ structure type with the tetragonal space group $P4/mbm$ and lattice parameters of approximately $a=12.5$ and $c=4.2$ Å (Fig. 1).[8,17] Although the structure has a unique axis it does not obviously exhibit low-dimensional features. It has been speculated that the chains of R atoms in the channels (the $R1$ atoms) carry a quasi-one-dimensional (1D) electron band. Deviations from tetragonal symmetry have not been found down to $T=2$ K, either in x-ray-powder diffraction or in the previous single-crystal diffraction experiments.[15]

Crucial to the discovery of the weak superlattice reflections in the x-ray diffraction was the availability of single crystals.[8] Temperature-dependent x-ray diffraction of $Lu_5Ir_4Si_{10}$ revealed the development of superlattice reflections below $T_{CDW}=83$ K. The positions of these satellite reflections could be described by the temperature-independent, commensurate modulation wave vector $\vec{q}=(0,0,\frac{3}{7})$. The intensities increased on decreasing temperature, however the increase was much more steep than it was expected for a second-order phase transition. This is in accordance with the sharp temperature dependencies of this transition observed in various physical properties.[8,12] Nevertheless, the transition appears continuous and without hysteresis in most experiments. Only recently a weak hysteresis was found at T_{CDW} in the temperature dependence of the ultrasound resonance frequencies.[9] The first-order character of the transition is in agreement with the commensurateness of the superstructure.

Single-crystal x-ray-diffraction experiments on $Er_5Ir_4Si_{10}$ revealed the presence of superlattice reflections below $T_{CDW}=151$ K. Commensurate ($\vec{q}=(0,0,\frac{1}{2})$) and incommensurate [$\vec{q}=(0,0,\frac{1}{4}\pm\delta)$ with $\delta\approx0.03$] satellites develop simultaneously, with intensities that increase on decreasing temperature approximately according to $(T_{CDW}-T)^{1/2}$, in agreement with a second-order phase transition. These results were interpreted by a model that invokes a structural transition at T_{CDW} towards a doubled unit cell, within which an incommensurate CDW develops.[11] This model was supported by the observation of diffuse scattering above T_{CDW} for the commensurate satellites only.[15] At $T_{lock\text{-}in}=55$ K a first-order lock-in transition was found, at which δ became zero. This fourfold, commensurate CDW then persists into the magnetically ordered state below $T_N=2.8$ K.

The temperature dependence of the satellite reflections in x-ray diffraction provided important information for the understanding of the phase transitions in compounds $R_5Ir_4Si_{10}$. The commensurate versus incommensurate character of the CDW explains that the transition in $Lu_5Ir_4Si_{10}$ is much sharper than the transition in $Er_5Ir_4Si_{10}$. Furthermore, it allows a lock-in transition to occur at $T_{lock\text{-}in}=55$ K in $Er_5Ir_4Si_{10}$, for which a counterpart has not been found in $Lu_5Ir_4Si_{10}$. Motivated by these successes, we have studied the temperature dependencies of the CDW satellite reflections in the x-ray diffraction of compounds $R_5Ir_4Si_{10}$ with R = Ho, Er, Tm, Lu, $Lu_{0.64}Er_{0.36}$, and $Lu_{0.84}Er_{0.16}$. The choice of compounds has been restricted to those compounds for which we were able to grow single crystals. Different types of superstructures have been found for different compounds. They allow us to rationalize the qualitatively different temperature dependencies of the physical properties in these compounds. Furthermore, a tentative (x,T) phase diagram will be constructed for the compounds $(Lu_{1-x}Er_x)_5Ir_4Si_{10}$.

II. EXPERIMENTAL

A. Growth of single crystals

Single crystals have been grown by a modified Czochralski technique according to procedures described elsewhere.[8,11] Starting materials were the high purity elements, which were mixed in the desired stoichiometry. The products were cylindrical bars with diameters of 3 mm and lengths between 30 and 40 mm. Electron microprobe analysis showed the compositions to be in accordance with the expected stoichiometry (accuracy 1%). Secondary phases occupied less than 2% of the volume. Single crystals of $R_5Ir_4Si_{10}$ have been made for R = Ho, Tm, $Lu_{0.34}Er_{0.66}$ ($x=0.66$), and $Lu_{0.16}Er_{0.84}$ ($x=0.84$). Material with R = Er, Lu was available from previous studies.[8,11]

B. Electrical conductivity

The dc electrical resistivity ρ was measured with a commercial physical properties measurement system by quantum design, employing the four-contact method. For $Tm_5Ir_4Si_{10}$ and $(Lu_{0.34}Er_{0.66})_5Ir_4Si_{10}$ pieces of single crystal of $\approx1.0\times1.0\times3.0$ mm^3 were cut out of the cylindrical bar. Contacts were made with copper wires and silver paint. Electrical resistances were measured along the $\vec{a}$ and $\vec{c}$ lattice directions for temperatures between 1.8 and 300 K. For $Tm_5Ir_4Si_{10}$ two transitions are visible as an anomalous upturn of the resistivity on cooling at temperatures equal to the transition temperatures determined by the x-ray diffraction (Fig. 2). The temperature dependence of the resistivity of

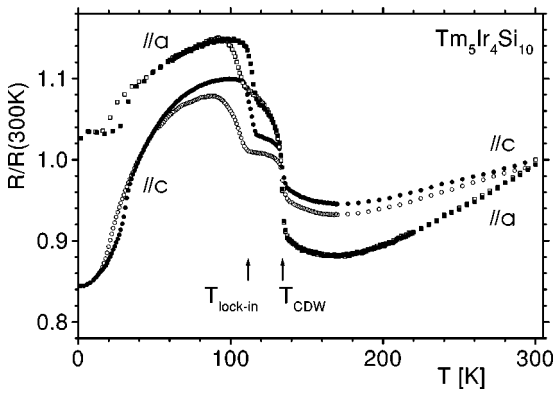

FIG. 2. Temperature dependence of the electrical resistance of $Tm_5Ir_4Si_{10}$ along the *c* axis (circles) and along the *a* axis (squares). The normalized resistance $[R(T)/R(T=300\ \mathrm{K})]$ is given for cooling (open symbols) and heating (filled symbols), with resistivities $\rho_a(300\ \mathrm{K})=1.884\mu\Omega$ m and $\rho_c(300\ \mathrm{K})=0.670\mu\Omega$ m. The transition temperatures as obtained by x-ray diffraction are marked by arrows.

$(Lu_{0.34}Er_{0.66})_5Ir_4Si_{10}$ shows a single transition at a temperature in accordance with the x-ray-diffraction results (Fig. 3). The absolute values of the resistivity show a relatively small anisotropy with higher values for the electrical resistance along $\vec{a}$.

For $Ho_5Ir_4Si_{10}$ and $(Lu_{0.16}Er_{0.84})_5Ir_4Si_{10}$ single crystals of sufficient sizes were not available for conductivity experiments. Instead, Fig. 4 shows the temperature dependence of the electrical resistivity of $Ho_5Ir_4Si_{10}$ and $(Lu_{0.12}Er_{0.88})_5Ir_4Si_{10}$ as measured on small bars of polycrystalline material. The behavior of $Ho_5Ir_4Si_{10}$ is similar to that of $Er_5Ir_4Si_{10}$, with an anomalous upturn at T_{CDW} and a restoration of the conductivity below $T_{lock\text{-}in}$.[11] $(Lu_{0.12}Er_{0.88})_5Ir_4Si_{10}$ exhibits similar behavior as $Tm_5Ir_4Si_{10}$ with an anomalous upturn of the resistivity at both transitions.

The temperature dependence of the resistivity as measured on polycrystalline material of $(Lu_{1-x}Er_x)_5Ir_4Si_{10}$

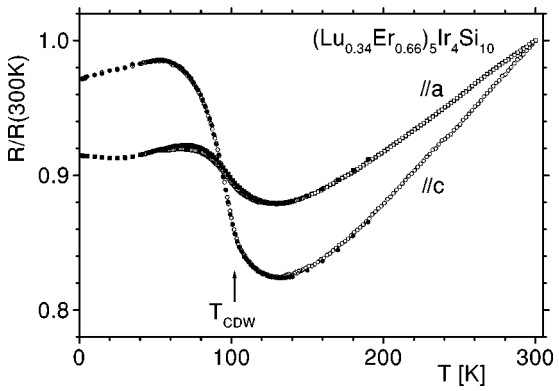

FIG. 3. Temperature dependence of the electrical resistance of $(Lu_{0.34}Er_{0.66})_5Ir_4Si_{10}$ along the *c* axis (circles) and along the *a* axis (squares). The normalized resistance $[R(T)/R(T=300\ \mathrm{K})]$ is given for cooling (open symbols) and heating (filled symbols). Resistivity values are not available. The transition temperature as obtained by x-ray diffraction is marked by an arrow.

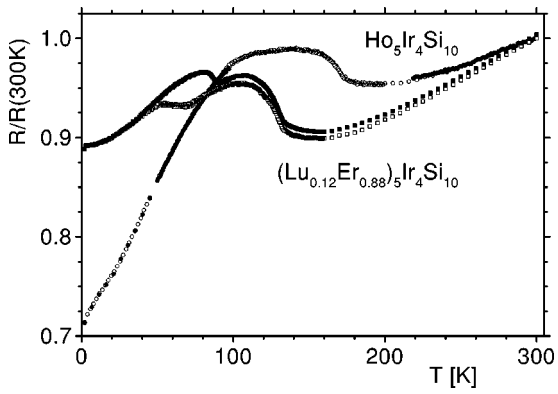

FIG. 4. Temperature dependence of the electrical resistivity of polycrystalline bars of $Ho_5Ir_4Si_{10}$ (circles) and $(Lu_{0.12}Er_{0.88})_5Ir_4Si_{10}$ (squares). The normalized resistance $[R(T)/R(T=300\ \mathrm{K})]$ is given for cooling (open symbols) and heating (filled symbols).

shows three types of behavior (data not shown; see Ref. 18). For $x=0$ the data show an upturn and a downturn, similar to the single-crystal data on $Er_5Ir_4Si_{10}$. For $0.66<x<0.88$ there is an upturn of the resistivity both at T_{CDW} and at $T_{lock\text{-}in}$ (Fig. 4), while for $0<x<0.60$ a single transition is observed similar to the single-crystal data in Fig. 3.

C. X-ray-diffraction experiments

Small pieces of approximate linear dimensions of 0.05 mm were broken off the cylindrical bars for single-crystal x-ray diffraction. Several pieces for each material were tested by measuring the diffraction on a NONIUS MACH3 four-circle diffractometer with rotating anode generator and Mo-$K\alpha$ radiation ($\lambda=0.7107$ Å). All pieces produced sharp Bragg reflections that could be indexed on the basis of the expected tetragonal unit cell. Lattice parameters were determined by the refinement against accurately measured positions of 25 reflections in four settings (Table I). It is noticed that the present values deviate from previously published values for R = Ho, Er, Tm, and Lu by up to 30 times the reported standard deviations.[8,7] These differences are attributed to systematic errors in the experiments. However, the relative values of the lattice parameters for different compounds as derived from experiments on a single instrument should be much more accurate, as is shown by the fact that

TABLE I. Tetragonal lattice parameters and volumes of the unit cell at room temperature for the compounds $R_5Ir_4Si_{10}$ with R = Er, Ho, Tm, Lu, $Lu_{0.34}Er_{0.66}$, and $Lu_{0.16}Er_{0.84}$. Standard uncertainties are given in parentheses.

R	a (Å)	c (Å)	V_{cell} (Å^3)
Ho	12.5338 (11)	4.2133 (5)	661.89 (11)
Er	12.5221 (7)	4.2042 (3)	659.23 (7)
Tm	12.4933 (7)	4.1911 (3)	654.16 (7)
Lu	12.4569 (7)	4.1709 (3)	647.22 (7)
$Lu_{0.34}Er_{0.66}$	12.4981 (7)	4.1908 (3)	654.62 (7)
$Lu_{0.16}Er_{0.84}$	12.5116 (6)	4.1973 (3)	657.05 (7)

similar trends have been found for Ho-Er-Tm by Yang *et al.*[7] and in the present experiment (Table I).

Different pieces gave Bragg reflections of different widths, whereby broader reflections indicate a poorer crystal quality. For all materials single crystalline pieces could be selected, for which the widths of reflections were equal to the instrumental width of 0.1° for the full width at half maximum (FWHM) for rotation of the crystal around the ω axis.

The closely related lattice parameters give sufficient evidence that each of the compounds crystallizes in the $Sc_5Co_5Si_{10}$ structure type (Table I).[17] Even stronger evidence can be obtained from refinements of the atomic coordinates against the integrated intensities of a complete set of Bragg reflections. Following this procedure, we have obtained a good fit of the $Sc_5Co_4Si_{10}$ structure type to the diffraction data of R = Er, Lu, and $(Lu_{0.34}Er_{0.66})$. In principle the degree of chemical order in $(Lu_{0.34}Er_{0.66})_5Ir_4Si_{10}$ can be determined by refinement of the ratio Lu/Er for each of the three crystallographically independent R sites. However, Lu and Er have nearly equal scattering powers, and they cannot be distinguished on the basis of the intensities obtained in an ordinary x-ray-diffraction experiment. Alternative experiments, such as resonant x-ray diffraction, are required to determine the chemical order. These experiments are beyond the scope of the present study. Nevertheless, it is noticed that complete chemical order in $(Lu_{1-x}Er_x)_5Ir_4Si_{10}$ can only exist, if x is exactly equal to 1/3 or 2/3.

Temperature-dependent x-ray diffraction was performed with synchrotron radiation at beamline D3 of Hasylab.[21] A wavelength of $\lambda = 0.5000$ Å was selected for R=Ho, Er, Tm, $Lu_{0.34}Er_{0.66}$, and $Lu_{0.16}Er_{0.84}$, while $\lambda = 0.63015$ for R=Lu. A closed-cycle helium cryostat manufactured by APD was used to set the temperature at different values between 20 and 300 K. The cryostat was mounted on a four-circle Huber diffractometer, allowing the setting angles of many different reflections to be measured. However, due to the bulky cryostat large regions of angles could not be reached. Because the crystals were not mounted in an orientated way, this forced us to select different reflections for the study of the satellite reflections of different crystals. Single-crystalline pieces were glued at the end of carbon fibers that themselves were glued to a copper block. The latter were attached to the cold finger of the cryostat, thus ensuring good thermal contact between crystal and cryostat.

For each crystal and each selected temperature, the orientation matrix was obtained from the setting angles of about 20 reflections. They were found to be in agreement with the expected tetragonal lattices. A possible splitting of reflections was not observed, again confirming the tetragonal lattice at all temperatures. The accuracy of the lattice parameters was less than with the MACH3 experiment, so that we refrain from an analysis of the thermal expansion.

The positions and intensities of possible superlattice reflections were obtained from q scans along the l direction (Fig. 5). The diffracted intensities were measured along the line $(h,k,l+\zeta)$ for $-0.1<\zeta<1.1$, and the positions of the reflections were obtained by fitting a pseudo-Voigt function for each observed diffraction maximum. The widths of the reflections vary between 0.001 and 0.010 FWHM in ζ. The

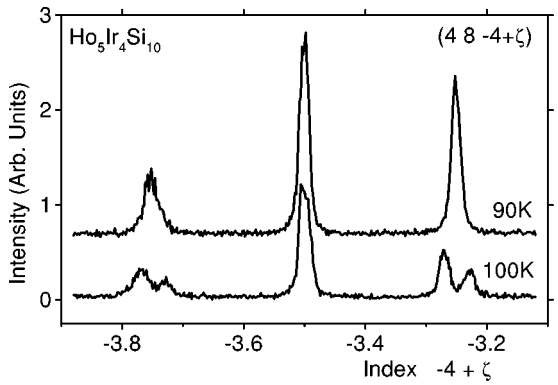

FIG. 5. q scans of the positions of the satellite reflections of $Ho_5Ir_4Si_{10}$ between $(4,8,-3.9)$ and $(4,8,-3.1)$. One scan in the incommensurate phase ($T=100$ K) and one scan below the lock-in transition ($T=90$ K) are shown.

different widths occurred for different reflections of each compound. In part they provide an explanation for the variations in accuracy with which positions and intensities of reflections could be measured. Small offsets of up to 0.01 along l were obtained for the positions of the main reflections (h,k,l) and $(h,k,l+1)$. The fitted positions of the superlattice reflections were corrected for these offsets.

For $Ho_5Ir_4Si_{10}$ q scans were performed for the reflections $(4,8,-4+\zeta)$, $(10,0,-3+\zeta)$ and $(10,0,-2+\zeta)$. The scan of $(4,8,-4+\zeta)$ below $T_{lock\text{-}in}$ clearly shows satellite reflections at $\zeta=0.25$, 0.5, and 0.75. $\lambda/2$ radiation as a possible origin of the maximum at $\zeta=0.5$ was excluded by the observation of this peak in a scan with a slightly detuned monochromator. The scan above $T_{lock\text{-}in}$ shows pairs of satellites at $\zeta=0.25\pm\delta$ and $0.75\pm\delta$ (Fig. 5). The positions of the satellites as derived from such scans at various temperatures are shown in Fig. 6. The best estimate for T_{CDW} is obtained from the extrapolation of the integrated intensities of the satellite reflections towards zero value (Fig. 7). The data are in good agreement with a $(T-T_{CDW})^{0.5}$ dependence, although it cannot be excluded that the intensity of the satellite at $(4,8,-3.5)$ increases more sharply on decreasing temperature below T_{CDW}. $T_{lock\text{-}in}$ is obtained less accurately with an estimated value in between the highest temperature with

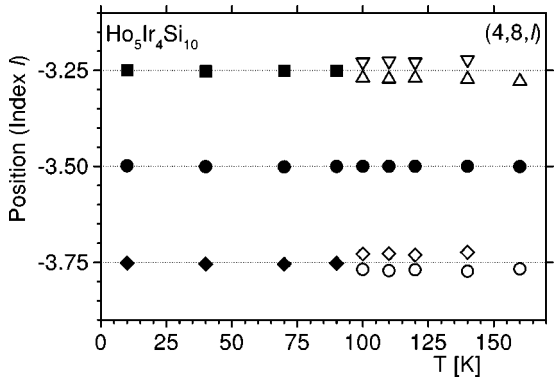

FIG. 6. Temperature dependence of the positions of the satellite reflections in the x-ray diffraction of $Ho_5Ir_4Si_{10}$ on the line $(4,8,-4+\zeta)$ with $0.1<\zeta<0.9$.

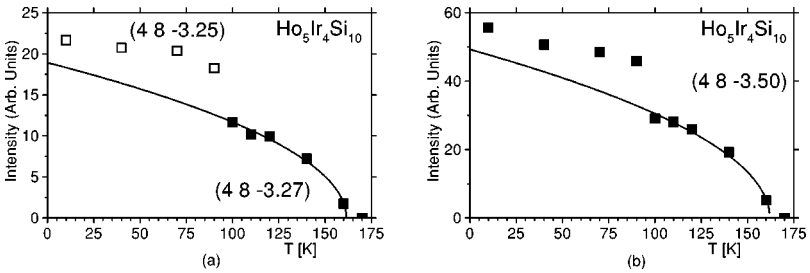

FIG. 7. Temperature dependence of the integrated intensities of satellite reflections of $Ho_5Ir_4Si_{10}$. The lines correspond to a fit of the function $I_0(T_{CDW}-T)^{1/2}$ to the data points between T_{CDW} and $T_{lock\text{-}in}$. (a) The reflections $(4,8,-3.25)$ (filled squares) and $(4,8,-3.27)$ (open squares) with $T_{CDW}=161.5(8)$ K. (b) The reflection $(4,8,-3.5)$ (filled squares) with $T_{CDW}=162.0(9)$ K.

commensurate satellites and the lowest temperature with incommensurate satellites (Table II). The deviation of the incommensurability parameter δ from the commensurate value of $\zeta=0.25$ of the positions of the incommensurate satellite reflections is about 0.025 and δ is weakly temperature dependent (Fig. 8), in accordance with the behavior of $Er_5Ir_4Si_{10}$.[11] The results on the scan of $(4,8,-4+\zeta)$ are confirmed by the two other scans, although in these cases the lower intensities lead to a lower accuracy.

For $Tm_5Ir_4Si_{10}$ q scans were performed for the reflection $(5,-12,\zeta)$. Scans at temperatures with $T_{lock\text{-}in}<T<T_{CDW}$ show a commensurate satellite reflection at $\zeta=0.5$ and incommensurate satellites at $\zeta=0.25\pm\delta$ and $\zeta=0.75\pm\delta$ [Fig. 9(a)]. Below $T_{lock\text{-}in}$ the pairs of incommensurate satellites are replaced by commensurate satellites at $\zeta=0.25$ and 0.75. In addition to these reflections other satellite reflections appeared at the positions given by $\zeta=0.125$, 0.375, 0.625, and 0.875 [Fig. 9(b)]. This implies that all superlattice reflections below $T_{lock\text{-}in}$ are at positions that can be indexed as $(h,k,l+n/8)$, where h, k, l, and n are integers. The deviation δ from the commensurate value of $\zeta=0.25$ depends more strongly on the temperature as for R = Ho, Er (Fig. 10). The temperature dependence of the intensity of the satellite at $(5,-12,0.5)$ has been fitted by the function $I_0(T_{CDW}-T)^{\beta}$. The fit for $\beta=0.5$ is not good, and the intensity increases more steeply than this function. A good fit to the data was obtained with a critical exponent of $\beta=0.29(2)$, resulting in $T_{CDW}=134.001(1)$ K (Fig. 11). $T_{lock\text{-}in}$ is again obtained as the value half way between the highest temperature with commensurate satellites and the lowest temperature with incommensurate satellites (Table II). The intensities of the satellite reflections are substantially lower in $Tm_5Ir_4Si_{10}$ than they are in $Ho_5Ir_4Si_{10}$ and $Er_5Ir_4Si_{10}$, with the result that the positions of the reflections and the value of δ could not be determined with the same accuracy as for the other compounds. A scan of $(1,-14,\zeta)$ showed only one of each pair of incommensurate satellites. Below $T_{lock\text{-}in}$ these scans did show satellites at $\zeta=0.25$, but the reflections at $\zeta=n/8$ (n is an odd integer) were missing. We believe that the failure to observe the additional satellites in these scans is due to the very small intensity of these reflections and the expected variations of intensities over reciprocal space.

For $(Lu_{1-x}Er_x)_5Ir_4Si_{10}$ $(x=0.84)$ q scans of the reflection $(4,8,-4+\zeta)$ at temperatures with $T_{lock\text{-}in}<T<T_{CDW}$ again show commensurate satellite reflections at $\zeta=0.5$ and incommensurate satellites at $\zeta=0.25\pm\delta_1$ and $\zeta=0.75\pm\delta_1$ (Fig. 12). Below $T_{lock\text{-}in}$ the pairs of incommensurate satellites are replaced by commensurate satellites at $\zeta=0.25$ and 0.75. In addition to these reflections other incommensurate satellite reflections appeared at positions $\zeta=0.125+\delta_2$, $\zeta=0.375\pm\delta_2$, $\zeta=0.625\pm\delta_2$, and $\zeta=0.875+\delta_2$. The temperature dependence of the incommensurability parameter δ_1 is similar to that of $Tm_5Ir_4Si_{10}$ [Fig. 13(a)]. The incommensurate splitting of the additional satellites below $T_{lock\text{-}in}$ is temperature independent at a value of approximately $\delta_2=0.01$ [Fig. 13(b)]. T_{CDW} is again determined by a fit to the intensities of the superlattice reflections (Fig. 14). These observations were confirmed by scans of the reflections $(4,10,-2+\zeta)$ and $(10,0,-3+\zeta)$. For the latter two scans incommensurate satellites were observed below $T_{lock\text{-}in}$ at $\zeta=0.375+\delta_2$ and $\zeta=0.625-\delta_2$ (Fig. 15). The fit with a single peak results in an incommensurate position in accordance with δ_2 derived from the $(4,8,-4+\zeta)$ scan.

TABLE II. Phase diagrams of the compounds $R_5Ir_4Si_{10}$ with R = Er, Ho, Tm, Lu, $Lu_{0.34}Er_{0.66}$, and $Lu_{0.16}Er_{0.84}$. All compounds are tetragonal $P4/mbm$ at room temperature. n denotes an integer. Standard deviations are given in parentheses. An accuracy of $\pm t$ indicates that incommensurate satellites were observed at $T_{lock\text{-}in}+t$, and that commensurate satellites were observed at $T_{lock\text{-}in}-t$.

R	T_{CDW} (K)	Modulation wave vectors	$T_{lock\text{-}in}$ (K)	Modulation wave vectors
Ho	161.4 (15)	$(0,0,\frac{1}{2})$ $(0,0,\pm\frac{1}{4}\pm\delta)$	90 ± 5	$(0,0,\frac{1}{2})$ $(0,0,\pm\frac{1}{4})$
Er[a]	151	$(0,0,\frac{1}{2})$ $(0,0,\pm\frac{1}{4}\pm\delta)$	55 ± 5	$(0,0,\frac{1}{2})$ $(0,0,\pm\frac{1}{4})$
Tm	134.1 (1)	$(0,0,\frac{1}{2})$ $(0,0,\pm\frac{1}{4}\pm\delta)$	111.5 ± 1.5	$(0,0,\frac{1}{2})$ $(0,0,\pm\frac{1}{4})$ $(0,0,n/8)$
Lu[b]	83	$(0,0,\pm n/7)$	–	
$Lu_{0.34}Er_{0.66}$	102.1 (21)	$(0,0,\pm n/7)$	–	
$Lu_{0.16}Er_{0.84}$	129.7 (12)	$(0,0,\frac{1}{2})$ $(0,0,\pm\frac{1}{4}\pm\delta_1)$	71 ± 2	$(0,0,\frac{1}{2})$ $(0,0,\pm\frac{1}{4})$ $(0,0,n/8\pm\delta_2)$

[a]Data from Ref. 11.

[b]Data from Ref. 8.

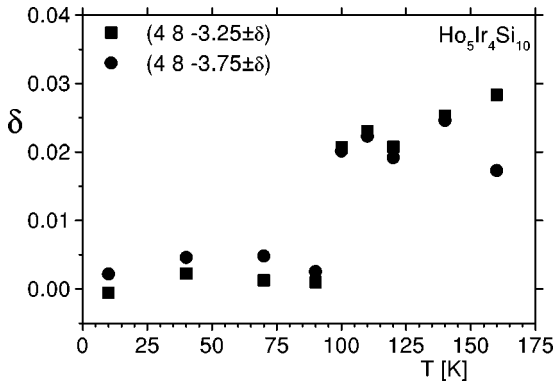

FIG. 8. Temperature dependence of the incommensurability parameter δ in $Ho_5Ir_4Si_{10}$. δ is obtained as half the distance between the pair of reflections $(48-3.25\pm\delta)$ (squares) and as half the distance between the pair of reflections $(48-3.75\pm\delta)$ (circles).

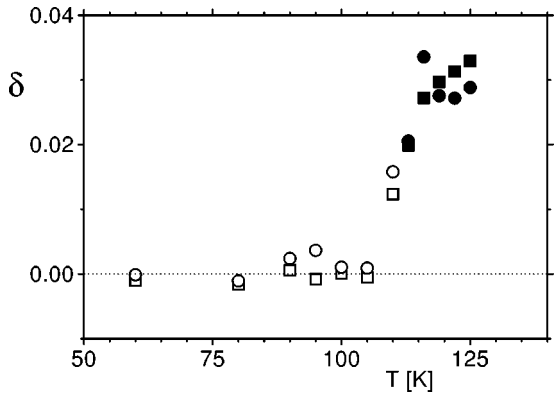

FIG. 10. Temperature dependence of the incommensurability parameter δ of $Tm_5Ir_4Si_{10}$. In the commensurate phase δ was obtained from the positions of the reflections $(5,-12,0.25-\delta)$ (open squares) and $(5,-12,0.75-\delta)$ (open circles); in the incommensurate phase δ was obtained from half the distance between $(5,-12,0.25\pm\delta)$ (filled squares) and from half the distance between $(5,-12,0.75\pm\delta)$ (filled circles).

These results give strong evidence that these satellites are incommensurate indeed [Fig. 13(b)].

The discovery of additional superlattice reflections below $T_{lock\text{-}in}$ persuaded us to study the compound $Er_5Ir_4Si_{10}$ again. At a temperature of 25 K several scans at position $(h,k,l+n/8)$ with $n=$ odd did not give any evidence for the presence of such reflections. Therefore we conclude that in $Er_5Ir_4Si_{10}$ these satellite reflections are not present indeed, in accordance with our previous experiment.[11]

For $(Lu_{0.34}Er_{0.66})_5Ir_4Si_{10}$ $(x=0.66)$ q scans were made of the reflections $(4,8,2+\zeta)$ and $(0,6,1+\zeta)$. They show commensurate satellite reflections at positions $\zeta=n/7$ with n an integer (Fig. 16). The positions are independent of the temperature. Due to a misjudgement at the time of this experiment, the q scans did not extend over the whole range of ζ. However, the positions $\zeta=\frac{2}{7}$, $\frac{3}{7}$, $\frac{4}{7}$, and $\frac{5}{7}$ are all present in the scans. They show that the intensities of the satellites at $\zeta=\pm\frac{2}{7}$ are higher than the intensities of the satellites at $\zeta=\pm\frac{3}{7}$. The temperature dependencies of the intensities of the satellite reflections were used to estimate $T_{CDW}=102.1(21)$ K of the single phase transition in this compound (Fig. 17).

Both compounds $(Lu_{1-x}Er_x)_5Ir_4Si_{10}$ with $x=0$ and $x=0.66$ exhibit a single phase transition towards a commensurate CDW with satellite reflections at positions $n/7$. A major difference between these compounds is the temperature dependence of the intensities of the satellite reflections that follows $(T_{CDW}-T)^{1/2}$ for $x=0.64$ (Fig. 17), but that is much sharper for $x=0$.[8] A second difference is that the strongest satellites in the compound $x=0.64$ are observed at $\zeta=\pm\frac{2}{7}$ (Fig. 16), while Becker *et al.*[8] report that the satellites at $\zeta=\pm\frac{3}{7}$ are much stronger than the other satellites, and they conclude towards a modulation wave vector of the CDW of $\vec{q}=(0,0,\frac{3}{7})$. We have studied the compound $Lu_5Ir_4Si_{10}$ again, and we could not confirm the observation by Becker *et al.*[8] A q scan of $Lu_5Ir_4Si_{10}$ along the line $(2,5,\zeta)$ did show satellites of comparable intensities at all positions $\zeta=n/7$ (Fig. 18). A data collection was made of the integrated intensities of all reflections up to $(\sin(\theta)/\lambda)_{max}=0.7$ Å^{-1}. The analysis showed that, on an average, the satellites with $\zeta=\pm\frac{2}{7}$ were almost twice as strong as those with $\zeta=\pm\frac{3}{7}$ or $\zeta=\pm\frac{1}{7}$. The most suitable choice for the commensurate modulation wave vector thus would be $\vec{q}=(0,0,\frac{2}{7})$ instead of $(0,0,\frac{3}{7})$ as it was proposed previously.[8]

Inspection of the data set of $Lu_5Ir_4Si_{10}$ showed that the satellite $(4,8,2+n/7)$ with $n=3$ is unobserved, but that the satellite with $n=4$ is only half as strong as the reflection at $n=2$. A similar intensity ratio for the compound $x=0.64$ would require the satellite at $(4,8,2+\frac{4}{7})$ to be observed, which it is not (Fig. 16). The intensities of the reflections $(0,6,1+n/7)$ in the compound $x=0$ with $n=3$, 4 are equal and they have values of half the intensity of the satellite at $n=2$. In the compound $x=0.64$ the satellites with $n=3$, 4 are observed, however with intensities much smaller than the intensity of the satellite $(0,6,2+\frac{2}{7})$. It can thus be concluded that evidence for a specific value of the CDW modulation wave vector is not available, because all satellites with $\zeta=n/7$ are observed. The limited scattering information on

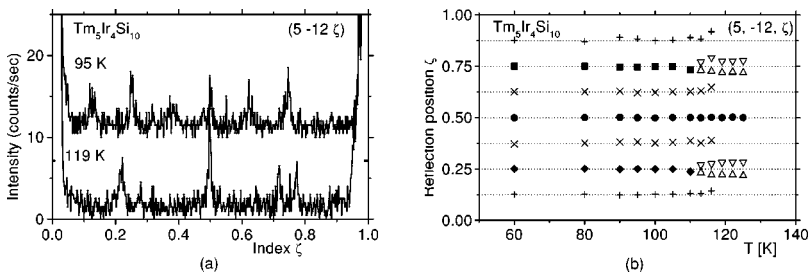

FIG. 9. Temperature dependence of the positions of the satellite reflections of $Tm_5Ir_4Si_{10}$ on the line $(5,-12,\zeta)$ with $0.1<\zeta<0.9$. (a) q scans at temperatures above $(T=119$ K) and below $(T=95$ K) the lock-in transition. (b) Temperature dependence of the positions of the satellites. Dashed lines indicate the positions $n/8$ with n an integer.

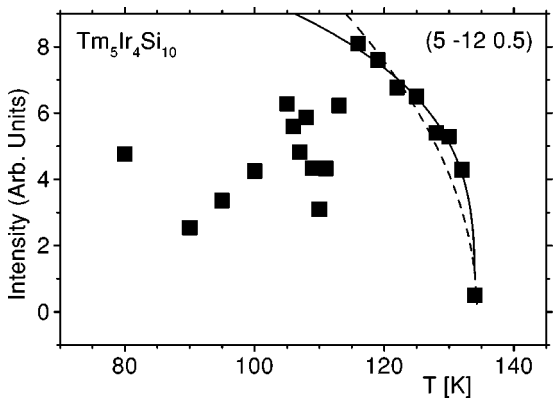

FIG. 11. Temperature dependence of the integrated intensities of the satellite reflection (5,−12,0.5) of $Tm_5Ir_4Si_{10}$. The lines correspond to a fit of the function $I_0(T_{CDW}-T)^{\beta}$ to the data points with $T_{lock\text{-}in}<T<T_{CDW}$. The full line for $\beta=0.29(2)$ and $T_{CDW}=134.001(3)$ K gives a much better description of the data than the dashed line with $\beta=\frac{1}{2}$ and $T_{CDW}=134.3(4)$ K.

$(Lu_{0.34}Er_{0.66})_5Ir_4Si_{10}$ suggests that in this compound the satellites with $\zeta=\pm\frac{2}{7}$ dominate the scattering much more than in $Lu_5Ir_4Si_{10}$.

III. DISCUSSION

A. The transition at T_{CDW}

On cooling from room temperature, the compounds $R_5Ir_4Si_{10}$ exhibit phase transitions at temperatures that we denote by T_{CDW} (Table II). At these temperatures physical properties, such as the electrical resistivity, specific heat, thermopower, and thermal conductivity, exhibit anomalies in their temperature dependence, which are in agreement with the loss of DOS at the Fermi level.[7,8,10] Single-crystal x-ray diffraction has revealed that superlattice reflections develop at T_{CDW}. The intensities of these satellites are several orders of magnitude lower than the intensities of the main reflections, in accordance with a very small distortion of the structure. These observations strongly support the original interpretation of these phase transitions as CDW transitions.[4]

Two classes of compounds can be distinguished on the basis of the positions of the satellite reflections: those with an incommensurate CDW (R=Ho, Er, Tm, and $Lu_{0.16}Er_{0.84}$) and those with commensurate superlattice reflections (R=Lu and $Lu_{0.34}Er_{0.66}$). This distinction explains the presence of a second transition in R=Ho, Er, Tm, and $Lu_{0.16}Er_{0.84}$ at which the incommensurate modulation becomes commensurate (lock-in transition; see below), while in compounds R=Lu and $Lu_{0.34}Er_{0.66}$ a second transition is not observed, because the CDW is already commensurate.

The incommensurability parameter δ behaves similarly in the different compounds. A value of ≈ 0.02 near $T_{lock\text{-}in}$ increases up to values between 0.03 and 0.04 at T_{CDW}, with a stronger temperature dependence for R=Tm and $Lu_{0.16}Er_{0.84}$ than for R=Ho and Er.

Although the transitions have been found to be continuous in almost all experiments, the critical exponents are different for different compounds. For the canonical second-order CDW phase transition, the temperature dependence of the intensities of the satellite reflections is expected to follow $I_0(T_{CDW}-T)^{\beta}$ with $\beta=\frac{1}{2}$. This value of β is approximately found for the compounds R = Ho, Er, and $Lu_{1-x}Er_x$ with $x=0.66$ and $x=0.84$ (Figs. 7, 14 and 17 and Ref. 11). The transitions in R = Tm and Lu are much steeper, with $\beta=0.3$ in $Tm_5Ir_4Si_{10}$ (Fig. 11).[8] The different characteristics of the CDW transitions, as observed by the temperature dependence of the intensities of the superlattice reflections, are in good agreement with the variation of widths of the transitions as determined from the temperature dependence of the specific heat.[10]

The sharpness of the transitions increases with the series Dy→Lu, i.e., with decreasing volume of the unit cell. However, the large width of the transitions in the mixed compounds $R=Lu_{1-x}Er_x$ shows that a simple relation between average ion size and width of the transition does not exist. Transitions towards incommensurate CDW's are expected to be of second order. Transitions towards commensurate CDW's can be weakly first order, in agreement with the observation of a small hysteresis in the temperature dependence of the resonance frequencies in ultrasound experiments.[9] In this respect, one would expect the transitions towards the commensurate CDW's to appear sharper than the transitions towards incommensurate CDW's, but this is not found. The two sharpest transitions occur for compounds with an incommensurate (R =Tm) and a commensurate (R = Lu) CDW, respectively, while the compound $Lu_{0.34}Er_{0.66}Ir_4Si_{10}$ has a broad transition towards a commensurate CDW. Apart from noting the variations in strength of the intrachain and interchain interactions that will exist for the different compounds, we do not have an explanation for the variation of widths of the CDW transitions.

Specific-heat measurements[10] and x-ray diffraction (Table II) have given values for T_{CDW} that differ up to 19 K. Both techniques have an uncertainty in the assignment of T_{CDW} that is smaller than 2 K. Therefore we attribute these differ-

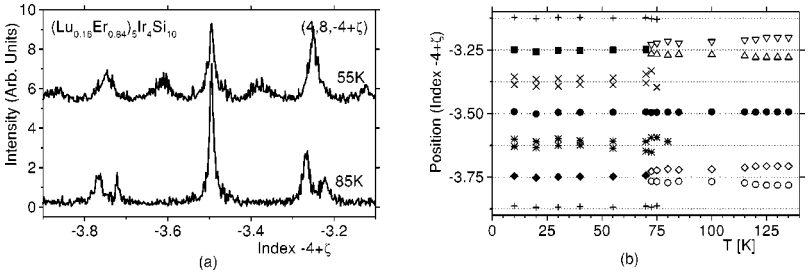

FIG. 12. Temperature dependence of the positions of the satellite reflections of $(Lu_{0.16}Er_{0.84})_5Ir_4Si_{10}$ on the line $(4,8,-4+\zeta)$ with $0.1<\zeta<0.9$. (a) q scans at temperatures above (T=85 K) and below (T=55 K) the lock-in transition. (b) Temperature dependence of the positions of the satellite reflections. Dashed lines mark the positions $n/8$.

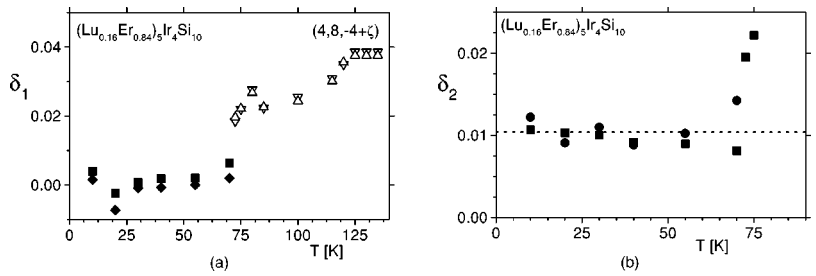

FIG. 13. Temperature dependence of the incommensurability parameters δ_1 and δ_2 of $(Lu_{0.16}Er_{0.84})_5Ir_4Si_{10}$. (a) δ_1 as defined by the positions of the reflections $(4,8,-3.25-\delta_1)$ (squares) and $(4,8,-3.75-\delta_1)$ (diamonds); in the incommensurate phase δ_1 was obtained as half the distance between the satellites at $(4,8,-3.25\pm\delta_1)$ (upright triangles) and those at $(4,8,-3.75\pm\delta_1)$ (down triangles). (b) Average values of δ_2 from the scans $(4,8,-4+\zeta)$ and $(4,10,-2+\zeta)$ for $0<\zeta<1$.

ences to the different behaviors of single crystals and polycrystalline samples, and the possible occurrence of impurity phases in the latter.

A linear dependence of T_{CDW} on the atom number has been suggested.[7,10] With the accurate values of T_{CDW} from x-ray diffraction we cannot confirm this observation (Table II). Alternatively, we find a linear dependence of T_{CDW} on the volume of the unit cell for the pure compounds with an incommensurate CDW (Fig. 19). The transition in $Lu_5Ir_4Si_{10}$ falls below this line, illustrating the different characters of the incommensurate and commensurate CDW's. The transition temperatures in the mixed compounds do not fit into this scheme, which can be explained by the influence of the chemical disorder on the transitions.

B. The lock-in transition

The compounds with an incommensurate CDW exhibit a second phase transition, at which the incommensurate CDW becomes commensurate. Previously this transition was found to be a pure lock-in transition in $Er_5Ir_4Si_{10}$, at which δ jumps to zero.[11] The same type of transition is presently found for $Ho_5Ir_4Si_{10}$. However, the lock-in transition is of different nature in the compounds with R=Tm and $Lu_{0.16}Er_{0.84}$. At T_{CDW} the incommensurate CDW becomes commensurate with $\delta_1=0$, similar to R = Ho and Er, but simultaneously new satellite reflections appear at commensurate positions $n/8$ in R = Tm or at incommensurate positions $n/8\pm\delta_2$ in $R=Lu_{0.16}Er_{0.84}$ (Table II). A correlation with the temperature dependence of the electrical resistivity is observed. In compounds R=Ho and Er the electrical resistivity makes a step downwards at $T_{lock\text{-}in}$, whereas in the compounds R=Tm and $Lu_{0.16}Er_{0.84}$ an anomalous increase of the resistivity is observed at $T_{lock\text{-}in}$. Thus in the compounds without an additional modulation part of the DOS at the Fermi level is restored, while in the other two compounds additional DOS is removed at the Fermi level.

These observations are in accordance with the development of a second CDW at $T_{lock\text{-}in}$. We propose a mechanism for this second CDW transition that is similar to the mechanism for the development of the high-temperature CDW in $Er_5Ir_4Si_{10}$.[11,15] The primary transition at $T_{lock\text{-}in}$ is a change of the modulation period of the high-temperature CDW towards the commensurate value of $\frac{1}{4}$. This period will not correspond to an optimal nesting condition, and part of the Fermi surface will be restored, in accordance with a decrease of the resistivity in R = Ho and Er at this temperature. Band-structure modifications due to the commensuration of the high-temperature CDW's then are responsible for favorable nesting conditions for the second CDW, as it develops in R =Tm and $Lu_{0.16}Er_{0.84}$. This second CDW removes more DOS at the Fermi level than there was restored by the commensuration of the high-temperature CDW, in accordance with an anomalous increase of the resistivity at $T_{lock\text{-}in}$ in R =Tm and $Lu_{0.16}Er_{0.84}$. Notice that this interpretation of the second transition differs from the mechanism recently proposed by Kuo *et al.*[10] Furthermore, the assignment of the transition at $T_{lock\text{-}in}=111.5$ K as the lock-in transition in $Tm_5Ir_4Si_{10}$ implies that a linear relation does not exist between $T_{lock\text{-}in}$ and the atom number or ionic size (Fig. 19).[10]

Resistivity data (Fig. 2) as well as the thermal conductivity[10] indicate a third transition in $Tm_5Ir_4Si_{10}$ at a temperature between 14 and 30 K, which is well above the transition temperatures of superconducting or magnetically ordered states in the other compounds. We can only speculate about the origin of this transition. It might be due to the development of magnetic order, or it might involve changes to the second CDW with period $n/8$.

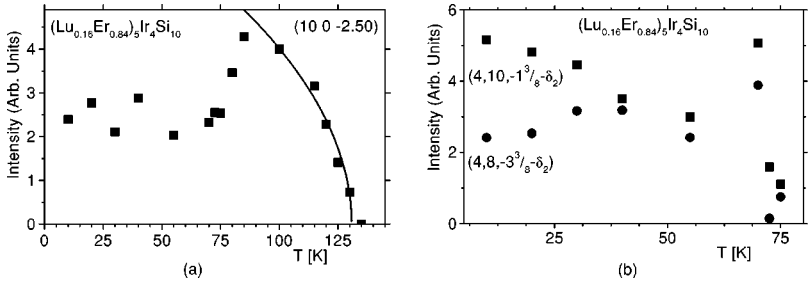

FIG. 14. Temperature dependence of the integrated intensities of satellite reflections of $(Lu_{0.16}Er_{0.84})_5Ir_4Si_{10}$. The lines correspond to a fit of the function $I_0(T_{CDW}-T)^{1/2}$ to the data points with $T_{lock\text{-}in}<T<T_{CDW}$. (a) The reflection $(10,0,-2.5)$. (b) The reflections $(4,10,-1-3/8-\delta_2)$ and $(4,8,-3-3/8-\delta_2)$.

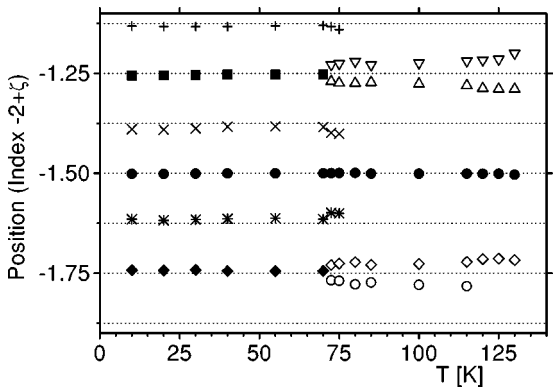

FIG. 15. Temperature dependence of the positions of the satellite reflections of $(Lu_{0.16}Er_{0.84})_5Ir_4Si_{10}$ on the line $(4,10,-2+\zeta)$ with $0.1<\zeta<0.9$. Dashed lines mark the positions $n/8$.

C. Phase transitions in mixed crystals $(Lu_{1-x}Er_x)_5Ir_4Si_{10}$

A tentative (x,T) phase diagram was constructed from the data on the transition temperatures of the compounds $(Lu_{1-x}Er_x)_5Ir_4Si_{10}$ (Fig. 20). It does not appear useful to describe the x dependence of T_{CDW} with a smooth curve over the whole range of x,[10] because the character of this transition changes from commensurate towards incommensurate for a composition between $x=0.66$ and $x=0.84$. In analogy with the sudden jump of δ towards the value 0 at T_{CDW}, it is expected that a critical composition (x_c) exists. For $x>x_c$ an incommensurate CDW and a lock-in transition will be found with $T_{CDW}>T_{lock\text{-}in}$, while for $x<x_c$ a single transition will occur towards a sevenfold supercell.

The presence of the CDW transition along the whole series $0<x<1$ is a further indication for unconventional behavior of the CDW's in compounds $R_5Ir_4Si_{10}$. Doping at the sites of the atoms carrying the 1D electron band, that is responsible for the CDW, usually suppresses the CDW transition for fractions of doping larger than $x=0.02$, while doping at sites not involved in the 1D band only weakly affects the CDW.[19,20] The different behavior of $R_5Ir_4Si_{10}$ compounds than that of canonical CDW systems might be due to

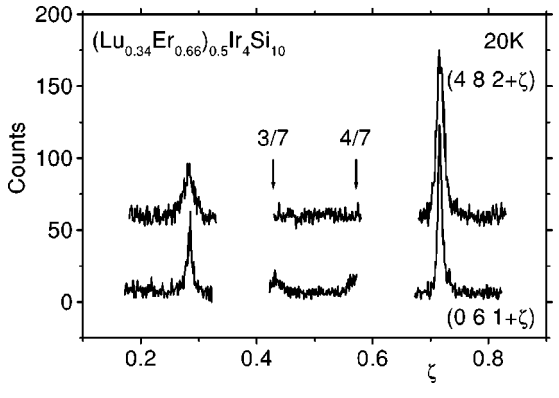

FIG. 16. Satellite reflections of $(Lu_{0.34}Er_{0.66})_5Ir_4Si_{10}$ at a temperature of $T=20$ K. q scans of the reflections $(4,8,2+\zeta)$ and $(0,6,1+\zeta)$ with $0.1<\zeta<0.9$ are shown. The data for $(4,8,2+\zeta)$ have been offset by 50 counts. The positions $\zeta=\frac{3}{7}$ and at $\zeta=\frac{4}{7}$ are marked by arrows.

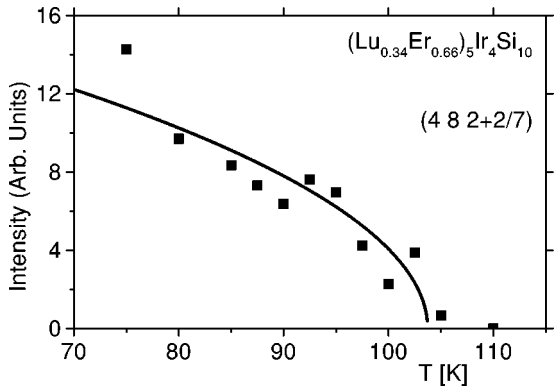

FIG. 17. Temperature dependence of the integrated intensities of the satellite reflection $(4,8,2+2/7)$ of $(Lu_{0.34}Er_{0.66})_5Ir_4Si_{10}$. The line corresponds to a fit of the function $I_0(T_{CDW}-T)^{1/2}$ with $T_{CDW}=103.7(15)$ K.

the different mechanism of pinning to impurities. In turn, a different mechanism of pinning might be the result of the strong interchain coupling as opposed to weak interchain coupling in the canonical CDW compounds. Alternatively, the observations on the doped compounds might be an indication that the doping does not affect the 1D electron bands. This would then imply that the chains of Ir or Si atoms carry the CDW.

IV. CONCLUSIONS

Temperature-dependent x-ray diffraction on compounds $R_5Ir_4Si_{10}$ has revealed an individual behavior for the compounds R = Ho, Er, Tm, Lu, and $(Lu_{1-x}Er_x)$ with $x=0.66$ and 0.84. The first distinction is the development of an incommensurate CDW in R = Ho, Er, Tm, and $Lu_{0.16}Er_{0.84}$ as opposed to a commensurate CDW in R = Lu and $Lu_{0.34}Er_{0.66}$. The compounds with an incommensurate CDW exhibit a pure lock-in transition for R = Ho and Er, while in other compounds a second CDW develops at $T_{lock\text{-}in}$, which is commensurate in R=Tm and incommensurate in $Lu_{0.16}Er_{0.84}$.

The simultaneous occurrence of commensurate and incommensurate satellite reflections at T_{CDW} has been inter-

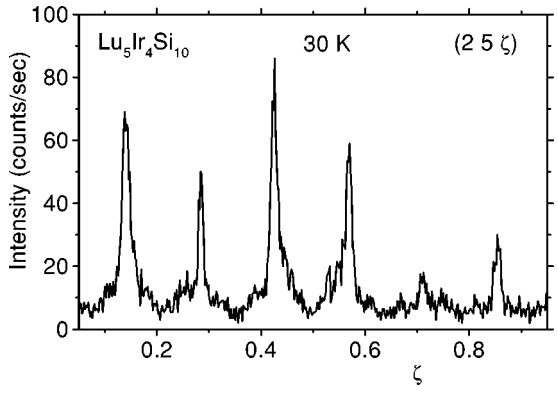

FIG. 18. Satellite reflections of $Lu_5Ir_4Si_{10}$ at $\zeta=n/7$ with n an integer in the q scan along the line $(2,5,0+\zeta)$ with $0.1<\zeta<0.9$.

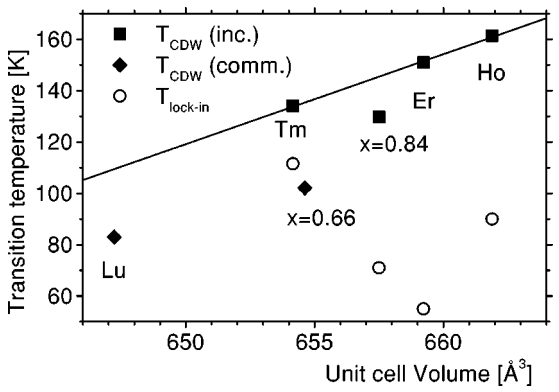

FIG. 19. Transition temperatures of compounds $R_5Ir_4Si_{10}$ as a function of the volume of the unit cell at room temperature. The line $(-2157.8+3.503\,V_{cell})$ is a fit to T_{CDW} of R=Tm, Er, and Ho.

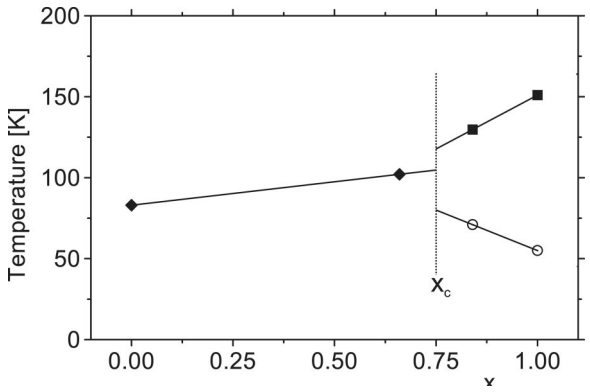

FIG. 20. Tentative (x,T) phase diagram of $(Lu_{1-x}Er_x)_5Ir_4Si_{10}$. Indicated are the transition temperatures towards the commensurate CDW (diamonds), the incommensurate CDW (squares), and the lock-in transition (circles). Lines are a guide for the eye. They illustrate the occurrence of a boundary between commensurate and incommensurate CDW's (critical concentration x_c). It is not suggested that the dependence of the transition temperatures on x would be linear.

preted by a mechanism comprising a structural phase transition towards a twofold superstructure, while the modified band structure of this superstructure then provides the proper nesting conditions for the incommensurate CDW.[11,15] The present results do not give any evidence to modify this interpretation.

We have discovered that at $T_{lock\text{-}in}$ additional superlattice reflections develop for R=Tm and $Lu_{0.16}Er_{0.84}$. A two-step mechanism is proposed for this transition that is similar to the mechanism for the transition at T_{CDW}. The commensuration of the high-temperature CDW leads to a modified band structure at $T_{lock\text{-}in}$, which then provides the proper nesting condition for a second CDW to develop at this temperature.

A tentative (x,T) phase diagram has been constructed for $(Lu_{1-x}Er_x)_5Ir_4Si_{10}$ from the observations of the transition temperatures in compounds with four different values of x. A critical concentration with $0.66<x_c<0.84$ is presumed at which the CDW switches between commensurate $(x<x_c)$ and incommensurate $(x>x_c)$.

ACKNOWLEDGMENTS

We are grateful to H.-G. Krane and C. Paulmann (Hasylab) and J. Lüdecke for assistance with the x-ray-diffraction experiments with synchrotron radiation. Synchrotron radiation diffraction experiments have been performed at beam line D3 of Hasylab (Hamburg, Germany). Financial support was obtained from the Deutsche Forschungsgemeinschaft (DFG) and the FCI.

*Electronic address: smash@uni-bayreuth.de; URL http://www.uni-bayreuth.de/departments/crystal/

†Also at the Max Planck Institute for Chemical Physics of Solids, 01187 Dresden, Germany.

[1] *Proceedings of the International Workshop on Electronic Crystals ECRYS-2002*, edited by S. Brazovskii, N. Kirova, and P. Monceau [J. Phys. IV France **12**, 9 (2002)].

[2] G. Gruner, *Density Waves in Solids* (Perseus Publications, Cambridge, 2000).

[3] J. Voit, Rep. Prog. Phys. **58**, 977 (1995).

[4] R.N. Shelton, L.S. Hausermann-Berg, P. Klavins, H.D. Yang, M.S. Anderson, and C.A. Swenson, Phys. Rev. B **34**, 4590 (1986).

[5] C.A. Swenson, R.N. Shelton, P. Klavins, and H.D. Yang, Phys. Rev. B **43**, 7668 (1991).

[6] K. Ghosh, S. Ramakrishnan, and G. Chandra, Phys. Rev. B **48**, 4152 (1993).

[7] H.D. Yang, P. Klavins, and R.N. Shelton, Phys. Rev. B **43**, 7688 (1991).

[8] B. Becker, N.G. Patil, S. Ramakrishnan, A.A. Menovsky, G.J. Nieuwenhuys, J.A. Mydosh, M. Kohgi, and K. Iwasa, Phys. Rev. B **59**, 7266 (1999).

[9] J.B. Betts, A. Migliori, G.S. Boebinger, H. Ledbetter, F. Galli, and J.A. Mydosh, Phys. Rev. B **66**, 060106 (2002).

[10] Y.K. Kuo, F.H. Hsu, H.H. Li, H.L. Huang, C.W. Huang, C.S. Lue, and H.D. Yang, Phys. Rev. B **67**, 195101 (2003).

[11] F. Galli, S. Ramakrishnan, T. Taniguchi, G.J. Nieuwenhuys, J.A. Mydosh, S. Geupel, J. Ludecke, and S. van Smaalen, Phys. Rev. Lett. **85**, 158 (2000).

[12] Y.K. Kuo, C.S. Lue, F.H. Hsu, H.H. Li, and H.D. Yang, Phys. Rev. B **64**, 125124 (2001).

[13] F. Galli, R. Feyerherm, R.W.A. Hendrikx, S. Ramakrishnan, G.J. Nieuwenhuys, and J.A. Mydosh, Phys. Rev. B **62**, 13 840 (2000).

[14] H.D. Yang, R.N. Shelton, and H.F. Braun, Phys. Rev. B **33**, 5062 (1986).

[15] F. Galli, R. Feyerherm, R.W.A. Hendrikx, E. Dudzik, G.J. Nieuwenhuys, S. Ramakrishnan, S.D. Brown, S. van Smaalen, and J.A. Mydosh, J. Phys.: Condens. Matter **14**, 5067 (2002).

[16] N.G. Patil and S. Ramakrishnan, Phys. Rev. B **59**, 9581 (1999).

[17] H.F. Braun, K. Yvon, and R. Braun, Acta Crystallogr., Sect. B: Struct. Crystallogr. Cryst. Chem. **36**, 2397 (1980).

[18] F. Galli, Ph.D. thesis, University of Leiden, The Netherlands, 2002.

[19] J. Ludecke, E. Riedl, M. Dierl, K. Hosseini, and S. van Smaalen, Phys. Rev. B **62**, 7057 (2000).
[20] D. Wang, Q. Xiao, W. Tang, T. Zhao, J. Shi, D. Tian, and M. Tian, Mod. Phys. Lett. B **13**, 109 (1999).
[21] A preliminary account of part of these results has been given at the ECRYS2002 meeting. See S. van Smaalen, P. Daniels, F. Galli, R. Feyerherm, E. Dudzik, G. J. Nieuwenhuys, and J. A. Mydosh, in *Proceedings of the International Workshop on Electronic Crystals ECRYS-2002* (Ref. 1), pp. 347–350.